⌘ *Author's Choice*

THE JOURNAL OF BIOLOGICAL CHEMISTRY VOL. 287, NO. 37, pp. 31406–31413, September 7, 2012
Published in the U.S.A.

Specialized Hsp70 Chaperone (HscA) Binds Preferentially to the Disordered Form, whereas J-protein (HscB) Binds Preferentially to the Structured Form of the Iron-Sulfur Cluster Scaffold Protein (IscU)*

Received for publication, February 13, 2012, and in revised form, June 11, 2012 Published, JBC Papers in Press, July 9, 2012, DOI 10.1074/jbc.M112.352617

Jin Hae Kim[‡], Marco Tonelli[§], Ronnie O. Frederick[¶], Darius C.-F. Chow[¶], and John L. Markley[‡§¶1]

From the [‡]Department of Biochemistry, [§]National Magnetic Resonance Facility at Madison, and [¶]Center for Eukaryotic Structural Genomics, University of Wisconsin, Madison, Wisconsin 53706

Background: IscU populates structured (S) and disordered (D) conformational states. In Fe-S cluster delivery, IscU interacts with HscB and HscA.
Results: NMR reveals differential interactions of the S- and D-states with HscA and HscB.
Conclusion: HscA and HscA-ADP bind preferentially to the D-state. HscB binds preferentially to the S-state. HscA-ATP binds neither the S- nor D-state tightly.
Significance: Fe-S cluster transfer is coupled to chaperone-mediated disordering of IscU.

The *Escherichia coli* protein IscU serves as the scaffold for Fe-S cluster assembly and the vehicle for Fe-S cluster transfer to acceptor proteins, such as apoferredoxin. IscU populates two conformational states in solution, a structured conformation (S) that resembles the conformation of the holoprotein IscU-[2Fe-2S] and a dynamically disordered conformation (D) that does not bind metal ions. NMR spectroscopic results presented here show that the specialized Hsp70 chaperone (HscA), alone or as the HscA-ADP complex, preferentially binds to and stabilizes the D-state of IscU. IscU is released when HscA binds ATP. By contrast, the J-protein HscB binds preferentially to the S-state of IscU. Consistent with these findings, we propose a mechanism in which cluster transfer is coupled to hydrolysis of ATP bound to HscA, conversion of IscU to the D-state, and release of HscB.

Fe-S clusters play key roles in all forms of life in functions as diverse as electron transport, enzyme activity, and environmental sensing. In the Fe-S cluster system for Fe-S cluster biosynthesis and delivery, which is conserved from prokaryotes (1) to the mitochondria of eukaryotes (2), Fe-S clusters are assembled on the scaffold protein IscU and are transferred to acceptor proteins through the agency of HscB, a J-protein co-chaperone, and HscA, a specialized Hsp70 chaperone (3). Cluster transfer involves ATP hydrolysis catalyzed by HscA attended by a change in the conformation of HscA (4). It is known that IscU and HscB bind to HscA and enhance its ATPase activity. However, the details of how these interactions are coupled to cluster transfer remain to be discovered.

Although IscU by itself has cluster transfer activity (5), the transfer rates are greatly stimulated in the presence of HscA, HscB, and MgATP (4). This indicates that HscA and HscB are required for efficient cluster transfer *in vivo*. It is intriguing that HscA and HscB are specifically used for Fe-S cluster transfer despite their high sequence identities to members of the Hsp70 and Hsp40 protein families: DnaK and DnaJ, respectively(6). As with other members of the Hsp70 and Hsp40 families, HscA has intrinsic ATPase activity, and this activity is greatly stimulated both by its protein substrate IscU and by HscB (7). In particular, the $L^{99}PPVK^{103}$ (*Escherichia coli* numbering) motif of IscU is recognized by HscA. The isolated nonapeptide $E^{98}LPPVKIHC^{106}$ is sufficient to stimulate the ATPase activity of HscA as much as full-length IscU (8, 9). HscA has two domains: the nucleotide-binding domain and the substrate-binding domain (SBD).[2] Nucleotide binding to the nucleotide-binding domain allosterically regulates the affinity of SBD for IscU (7). The dissociation constant for apo-IscU bound to HscA-ATP is 37 μM, whereas it is 9 μM for apo-IscU bound to HscA-ADP (10). As with Hsp40 proteins, HscB has an N-terminal J-domain that interacts with HscA by a highly conserved His-Pro-Asp motif and a C-terminal domain that binds IscU (11, 12). The dissociation constant between HscB and apo-IscU was reported to be ~13 μM (11).

The discovery of a disease caused by an intronic mutation in the human *ISCU* gene (13, 14) has demonstrated the critical role of the scaffold protein (IscU) encoded by this gene. More recently, it was found that complete knock-out of the *Iscu* gene in mice results in early embryonic death (15).

We have shown that apo-IscU populates two interconverting conformational states, a disordered (D) state and a structured

* This work was supported, in whole or in part, by National Institutes of Health Grants R01 GM58667 and U01 GM94622 in collaboration with the National Magnetic Resonance Facility at Madison, which is supported by NIH grants from the National Center for Research Resources (5P41RR002301-27 and RR02301-26S1) and the National Institute for General Medical Sciences (8 P41 GM103399-27).
⌘ *Author's Choice*—Final version full access.
The assignments reported in this paper have been deposited in the Biological Magnetic Resonance Data Bank with accession number 18381.

[1] To whom correspondence should be addressed: Dept. of Biochemistry, University of Wisconsin, 433 Babcock Dr., Madison, WI 53706. Tel.: 608-263-9349; Fax: 608-262-3759; E-mail: jmarkley@wisc.edu.

[2] The abbreviations used are: SBD, substrate-binding domain; D, disordered; S, structured; TROSY, transverse relaxation optimized spectroscopy; HSQC, heteronuclear single quantum correlation.

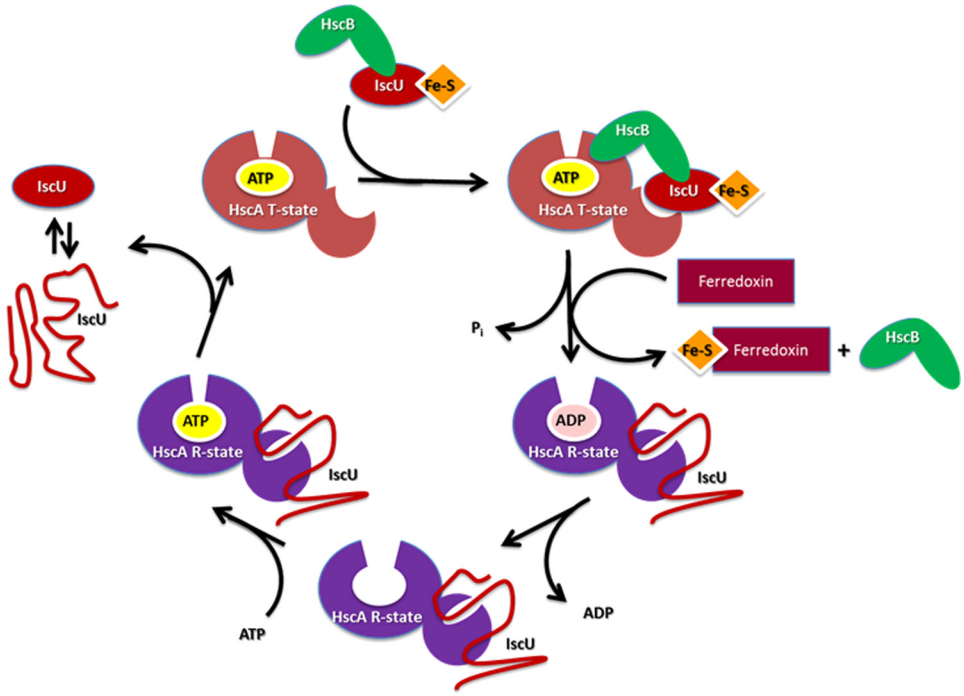

FIGURE 1. **Current working model of the Fe-S cluster transfer mechanism.** The cycle initiates with recruitment of the complex between HscB (*green*) and Fe-S cluster-bound IscU (IscU, *red*; Fe-S cluster, *orange*) to ATP-bound HscA (T-state; *tan*). An acceptor protein, represented here by ferredoxin (*maroon*), attacks the cluster, leading to hydrolysis of ATP and a concomitant conformational change in ADP-bound HscA (R-state; *purple*), which stabilizes the disordered form of IscU. Disordering of IscU leads to release of the cluster and HscB. Disordered IscU remains bound to HscA after release of ADP, but subsequent binding of ATP changes the conformation of HscA to the T-state, which releases apo-IscU. This scheme incorporates the findings reported here into earlier mechanisms (4, 7). Specifically, the current mechanism shows cluster transfer coupled to attack by the acceptor protein, ATP hydrolysis, the T-to-R conformational change of HscA, and the conversion of IscU from the S- to D-state, with release of the cluster and HscB.

(S) state, and that interaction with HscB shifts the D ⇄S equilibrium toward the S-state (16). The structure of the S-state resembles that adopted by IscU when it contains either a [2Fe-2S] cluster (17) or Zn^{2+} ion (18), whereas the D-state appears not to interact with metal ions (19). We report here that the addition of a substoichiometric quantity of HscA decreases the D → S rate while not affecting the S → D rate, thus shifting the D ⇄ S equilibrium toward the D-state. In the presence of excess HscA or the HscA-ADP complex, IscU becomes transformed to a D-like state. By contrast, a variant of IscU that exists predominantly in the S-state (N90A) and the IscU-Zn^{2+} complex that is fully in the S-state (19) are each only partially converted to the D-like state upon the addition of HscA. These results suggest that HscA, alone or as the ADP complex, binds to and stabilizes the D-state of IscU. The addition of ATP to the IscU-HscA complex causes release of IscU, which then resumes the D ⇄ S equilibrium. We propose a mechanism (Fig. 1) consistent with these findings in which cluster transfer from IscU is coupled to hydrolysis of HscA-bound ATP and the concomitant conformational change that enables HscA-ADP to bind and stabilize the D-state of IscU, which promotes both the release of the Fe-S cluster to an acceptor protein and the release of HscB.

EXPERIMENTAL PROCEDURES

Production and Purification of Proteins—HscB, [U-^{15}N]apo-IscU, and [U-^{13}C,^{15}N]apo-IscU were prepared as described previously (11, 16). [U-^{15}N,frac-^{2}H]Apo-IscU (where frac-^{2}H indicates fractionally ^{2}H-labeled) was produced as follows. First, a single colony of transformed BL21 competent cells (Novagen) was transferred to 5 ml of LB medium containing 100 μg/ml ampicillin and incubated for ~8 h at 37 °C. From this, a 0.1-ml inoculum was transferred to 5 ml of M9 minimal medium supplemented with 100 μg/ml ampicillin, 1 g/liter NH_4Cl, and 5 g/liter glucose. The cells were adapted to growth in D_2O by stepwise growths of 0.1-ml inoculants in 5 ml of M9 medium dissolved in 20, 50, 80, and 100% D_2O, respectively; each cell growth was incubated for 8–12 h at 37 °C. A 0.1-ml inoculant from 5 ml of 100% D_2O/M9 medium was transferred to 50 ml of 100% D_2O/M9 medium, which was incubated for ~20 h at 37 °C. The cell pellet harvested from 50 ml of medium was finally transferred to 500 ml of 100% D_2O/M9 medium supplemented with 100 μg/ml ampicillin, 1 g/liter $^{15}NH_4Cl$, and 5 g/liter glucose. Overexpression was induced by the addition of 0.4 mM isopropyl β-D-thiogalactopyranoside at $A_{600} \approx$ 0.8, followed by further incubation for 6–8 h at 37 °C. This procedure, which leads to the deuteration of most H^{α} and H^{β} positions, results in significant increases in the intensities of $^{1}H^{N}$ signals from larger macromolecules (20). Harvested cell pellets were stored at −80 °C until used.

The expression plasmids for full-length WT HscA and the HscA SBD (residues 389–616) were generous gifts from Dr. Larry E. Vickery (University of California, Irvine). The expression plasmid for HscA(T212V) was created by applying the QuikChange II site-directed mutagenesis kit (Stratagene) to the WT HscA expression vector. Full-length HscA and the HscA SBD were produced by procedures described previously (21, 22).

Full-length HscA and the HscA SBD were purified by procedures described previously (21, 22), except for the use of anion-exchange chromatography and size-exclusion chromatography instead of reversed-phase chromatography. For the additional anion-exchange chromatography step, a DEAE Bio-Gel column (Bio-Rad) was used with a 0–0.15 M NaCl gradient. Size-exclusion chromatography was accomplished with a HiLoad 16/60 Superdex 200 column (GE Healthcare) for full-length HscA or with a HiLoad 16/60 Superdex 75 column (GE Healthcare) for the HscA SBD. The elution buffer for this step consisted of 50 mM Tris-HCl (pH 7.5), 1 mM DTT, 0.5 mM EDTA, and 150 mM NaCl.

NMR Spectroscopy—The solvent used for NMR samples contained either 50 mM HEPES/NaOH (pH 7.3), 10 mM $MgCl_2$, 150 mM KCl, and 5 mM DTT (HMKD buffer) or 50 mM Tris-HCl (pH 7.5), 0.5 mM EDTA, and 5 mM DTT (TED buffer) with 7% D_2O, 0.7 mM 2,2-dimethyl-2-silapentane-5-sulfonate, and 0.02% sodium azide. All NMR spectra were acquired on 600- or 900-MHz Varian VNMRS spectrometers equipped with a *z*-gradient cryogenic probe. Sample temperatures were maintained at 25 °C. NMRPipe (23) was used to process the raw NMR data; SPARKY (24) was used for data analysis; and the Newton software package (25) was used to determine peak volumes and their ratios.

The titration experiments of IscU and IscU(N90A) were initiated with 0.3 mM [U-^{15}N]apo-IscU samples in HMKD buffer, and these samples were subsequently mixed with 1 or 2 eq of unlabeled full-length HscA or the HscA SBD. A two-dimensional ^{15}N transverse relaxation optimized spectroscopy-heteronuclear single quantum correlation (TROSY-HSQC) spectrum of each mixture was collected. For the titration experiment with WT IscU-Zn^{2+}, the complex was prepared by adding $ZnCl_2$ (final concentration of 1 mM) to the protein sample. The chemical shift perturbation of apo-IscU upon interacting with HscA was investigated by titrating [U-^{13}C,^{15}N]apo-IscU with unlabeled WT HscA and collecting three-dimensional HNCO spectra. Combined ^{1}H and ^{15}N chemical shift changes of ^{1}H-^{15}N cross-peaks were calculated as follows: $\Delta\delta_{NH} = ((\Delta\delta_N/6)^2 + (\Delta\delta_H)^2)^{1/2}$. The backbone NMR signals from [U-^{13}C,^{15}N]apo-IscU mixed with 2-fold unlabeled HscA were assigned by analyzing two-dimensional ^{15}N TROSY-HSQC, three-dimensional HNCO, three-dimensional HN(CO)CA, and three-dimensional HNCACB spectra with reference to assigned chemical shifts of the D-state of IscU (19).

The conformational exchange rates of apo-IscU were measured by two-dimensional NMR exchange spectroscopy (26). To achieve this, we prepared samples containing 0.35 mM [U-^{15}N]apo-IscU in TED buffer alone and in the presence of a substoichiometric amount (0.09 mM) of added HscA. Two-dimensional N_z exchange ^{15}N HSQC spectra were collected for each sample with a series of mixing times: 0, 20, 40, 60, 80, 100, 200, and 300 ms. The rates of the conformational transition were estimated from the initial slopes of the exchange cross-peak volumes normalized by the diagonal peak volumes as a function of the mixing time (≤200 ms) (26). No exchange cross-peaks were observed with mixing times of 0 and 20 ms, whereas with mixing times longer than 200 ms, the slopes were no longer linear as the result of relaxation effects. Previous NMR peak assignments to residues of apo-IscU in the S- and D-states (19) were used in obtaining residue-specific exchange rates. The experiments were repeated twice with two independently prepared samples to estimate errors from S.D.

Determination of the conformational states of apo-IscU under various conditions was accomplished by monitoring the volumes of the Lys-128 ^{1}H-^{15}N peaks: δ_H 7.76 ppm and δ_N 126.2 ppm in the S-state and δ_H 7.85 ppm and δ_N 126.2 ppm in the D-state. Measurements were initiated with samples of 0.3 mM [U-^{15}N]apo-IscU in HMKD buffer. To produce the complexes, we added 0.3 mM HscB, 0.3 mM HscA, or 0.3 mM HscA(T212V). We subsequently added 10 mM ADP or 10 mM ATP. The intensities of the Lys-128 S- and D-state ^{1}H-^{15}N peaks were measured from two-dimensional ^{15}N TROSY-HSQC spectra of each mixture. Nucleotide exchange on HscA has been shown to be fast and not to require an exchange factor (27). As a model for HscA bound to ATP, we used the HscA(T212V)-ATP complex because this variant exhibits negligible (if any) ATPase activity, yet it undergoes the nucleotide-induced conformational transition (28–30).

RESULTS

HscA Binds and Stabilizes the Disordered State of Apo-IscU—To determine whether HscA interacts preferentially with the S- or D-state of IscU, we used two-dimensional ^{1}H-^{15}N exchange spectroscopy to compare the S → D and D → S conformational exchange rates of [U-^{15}N]apo-IscU in the absence and presence of substoichiometric HscA. In this experiment, the exchange peak horizontal to the S diagonal peak reports on the S → D reaction, and the exchange peak horizontal to the D diagonal peak reports on the D → S reaction (Fig. 2*A*). We measured the ratio of the cross-peak to the diagonal as a function of the mixing time of the experiment and determined the rate from the initial slope before exchange became obscured by relaxation effects (Fig. 2*B*) (26). We found that the addition of 0.25 eq of HscA reduced the D → S rate by a factor of ~2 (Fig. 2*B*, *lower panels*), whereas the S → D rate was unaffected within experimental error (Fig. 2*B*, *upper panels*). The addition of ADP did not induce further change in the exchange rate of IscU (data not shown). This result suggests that HscA preferentially interacts with and stabilizes the D-state of apo-IscU.

We used two-dimensional ^{15}N TROSY-HSQC spectroscopy to follow the titration of a sample of [U-^{15}N]apo-IscU with increasing amounts of unlabeled HscA. Before the addition of HscA, the spectrum (Fig. 3*A*) exhibited sets of peaks corresponding to those assigned to the S- and D-states of IscU (16, 19). Upon the addition of HscA, the peaks corresponding to the S-state decreased progressively and had nearly disappeared at a level of 2 eq of unlabeled HscA/eq of ^{15}N-labeled IscU; only peaks corresponding to a D-like state remained (Fig. 3*B*). The subsequent addition of 2 eq of unlabeled IscU led to partial recovery of signals corresponding to the S-state (Fig. 3*C*) as the result of displacing some of the ^{15}N-labeled IscU from the IscU-HscA complex; this result shows that the IscU-HscA interaction is reversible and that the observed effects were not the result of an artifact such as irreversible protein denaturation or proteolysis. The side chain ^{1}H-^{15}N of Trp-76 (the only tryptophan residue in IscU) exhibited separate two-dimensional

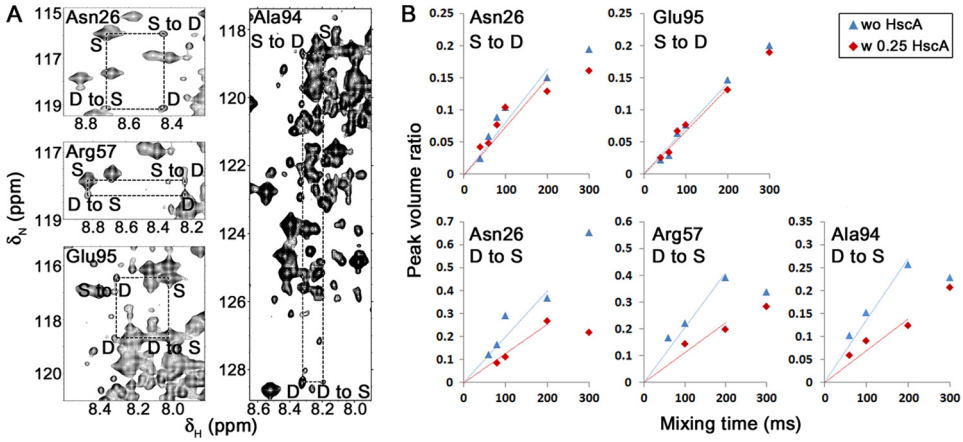

FIGURE 2. **Effect of the addition of a substoichiometric amount of HscA on the exchange rates linking the S- and D-states of [U-^{15}N]apo-IscU as determined by two-dimensional ^{1}H-^{15}N NMR exchange spectroscopy.** *A*, regions of the ^{1}H-^{15}N NMR exchange spectrum of [U-^{15}N]apo-IscU exhibiting signals from Asn-26, Arg-57, Ala-94, and Glu-95. Diagonal peaks corresponding to the S- and D-states of apo-IscU are labeled *S* and *D*, respectively, and peaks denoting the exchange from the S- to D-state and from the D- to S-state are labeled *S to D* and *D to S*, respectively. *B*, *upper panels*, plots of the ratio of the volume of the cross-peak representing the S → D reaction to the volume of its diagonal as a function of the mixing time; *lower panels*, plots of the ratio of the volume of the cross-peak representing the D → S reaction to the volume of its diagonal as a function of the mixing time. The *straight lines* represent the initial slopes, which yield the rates. The peaks studied were chosen because they were not overlapped by other signals. Both cross-peaks and diagonals were observable for Asn-26, but only single cross-peaks and diagonals were observable for the other residues. The agreement of the measured rates within experimental error is consistent with a two-state reaction. In the absence of HscA (*wo HscA*; *blue triangles*), the S → D (*upper panels*) exchange rates were 0.75 ± 0.07 s^{-1} for Asn-26 and Glu-95, and the D → S (*lower panels*) exchange rates were 2.15 ± 0.21 s^{-1} for Asn-26, 2.25 ± 0.21 s^{-1} for Arg-57, and 1.7 ± 0.42 s^{-1} for Ala-94. In the presence of 0.25 eq of HscA (*w 0.25 HscA*; *red diamonds*), the S → D rate remained unchanged within experimental error, whereas the D → S rate decreased to 1.1 ± 0.28 s^{-1} for Asn-26, 1.0 ± 0.14 s^{-1} for Arg-57, and 0.65 ± 0.07 s^{-1} for Ala-94. The addition of excess ADP to the samples did not perturb the exchange rates. This indicates that HscA preferentially interacts with and stabilizes the D-state of IscU.

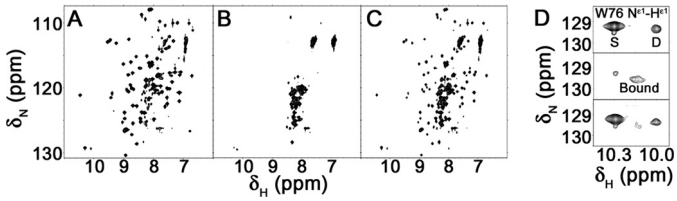

FIGURE 3. **Interaction with HscA stabilizes the D-state of IscU.** *A*, two-dimensional ^{15}N TROSY-HSQC spectrum of [U-^{15}N]apo-IscU in the absence of HscA. *B*, spectrum of the sample shown in *A* following the addition of 2 eq of unlabeled HscA. *C*, spectrum of the sample shown in *B* following the addition of 2 eq of unlabeled apo-IscU. *D*, expansions of the spectral regions from *A*–*C* containing the ^{1}H-^{15}N signals from the side chain of Trp-76 in the S- and D-states are shown in the *upper*, *middle*, and *lower panels*, respectively.

NMR cross-peaks for the S- and D-states (Fig. 3, *A* and *D*, *upper panel*). Upon formation of the IscU-HscA complex, the signals assigned to the S- and D-states decreased in intensity, and a new peak grew in intensity at an intermediate position (Fig. 3*D*, *middle panel*). The new signal corresponds to Trp-76 of IscU in the IscU-HscA complex. Given the size of the IscU-HscA complex (79.5 kDa), the fact that the IscU ^{1}H-^{15}N cross-peaks are relatively sharp indicates that they arise from disordered regions of the protein. These results confirm that HscA interacts preferentially with the D-state of IscU and stabilizes a D-like state in the complex.

We were able to assign a large number of backbone signals in spectra of the IscU-HscA complex by collecting three-dimensional HNCO spectra of [U-^{13}C,^{15}N]apo-IscU as a function of added HscA (Fig. 4*A*). These assignments, which we have deposited in the Biological Magnetic Resonance Data Bank (accession number 18381), enabled us to compare the chemical shifts of the ^{1}H-^{15}N backbone signals of the IscU-HscA complex with those assigned to the S- and D-states of apo-IscU alone (19). We found that the signals from the complex closely resembled those of the free D-state. This is illustrated in Fig. 4*B*, which plots the difference of the combined ^{1}H and ^{15}N chemical shifts of the complex minus those of the free D-state as a function of residue number. The chemical shift differences were all <0.025 ppm with the exception of the 0.04 ppm shift of Glu-95, a residue that flanks the L^{99}PPVK^{103} motif (Fig. 4*B*). Signals corresponding to Val-73–Val-77, Gly-79, Glu-96, Val-102, Ile-108, Ala-110, Asp-112, Ala-117, and Lys-122 (indicated by *red* × in Fig. 4*B*) broadened as HscA was added and were no longer detected after the addition of a stoichiometric amount of HscA. The broadening likely arises from residues becoming immobilized by binding to HscA, and this conclusion is reinforced by the fact that several of the broadened signals correspond to residues flanking the L^{99}PPVK^{103} motif of IscU, which is known to interact with HscA (8, 9, 22). Chemical shift analysis of the assigned signals from IscU complexed with HscA showed that the protein lacks secondary structure (Fig. 4*C*). From these results, we conclude that the conformation of IscU bound to HscA closely resembles that of the D-state of free apo-IscU, which is dynamically disordered and exhibits no secondary structural elements (19). To illustrate this, on the three-dimensional structure of the S-state of IscU (Fig. 4*D*), residues of IscU shown to be disordered in the IscU-HscA complex are colored *green*, and residues whose signals broadened in the IscU-HscA complex are colored *red*; residues shaded *black* are ones whose signals were not observed in the spectrum of free IscU.

Because the S-state of apo-IscU is known to be stabilized by the N90A substitution (19) or by the addition of Zn^{2+} (16, 19), we investigated the effects of adding HscA on the conformations of these two proteins. In comparison with wild-type IscU, much more of the S-state remained after the addition of 2 eq of HscA to [U-^{15}N]apo-IscU(N90A) or to [U-^{15}N]IscU-Zn^{2+} (data not shown). These results indicate that HscA does not

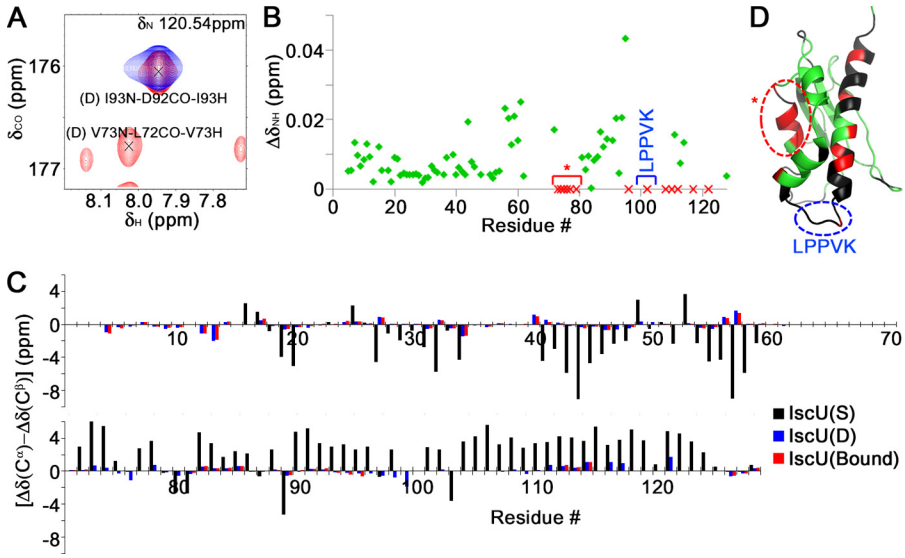

FIGURE 4. **Changes in the two-dimensional ^{1}H-^{15}N spectrum of IscU upon the addition of HscA.** *A*, representative examples of D-state signals from [U-^{13}C,^{15}N]apo-IscU that are perturbed upon the addition of HscA. Shown is a two-dimensional ^{1}H-^{13}C slice through a three-dimensional HNCO spectrum at the ^{15}N chemical shift shown at the top of the panel (120.54 ppm). The spectrum of [U-^{13}C,^{15}N]apo-IscU alone (*red*) is overlaid with the spectrum of [U-^{13}C,^{15}N]apo-IscU-HscA (1:2; *blue*). The signal from Val-73 has disappeared in the spectrum of the complex, whereas that from Ile-93 is unperturbed. *B*, absolute value of the change in the combined ^{1}H-^{15}N chemical shift of NMR signals corresponding to the D-state of IscU upon the addition of 2 eq of HscA plotted as a function of the residue number. Residues whose signals were observed initially but broadened and were no longer observed in the IscU-HscA complex are indicated (*red* ×). The L^{99}PPVK^{103} motif known to interact with HscA (8, 9) is indicated in *blue*, and the V^{73}TEWVKG^{79} motif that is proposed in this study as an additional recognition site is marked with an *asterisk*. *C*, secondary NMR chemical shifts ($\Delta\delta_{C\alpha} - \Delta\delta_{C\beta}$) of IscU bound to HscA (*red bars*) are compared with those of apo-IscU in the structured (*IscU(S)*; *black bars*) and disordered (*IscU(D)*; *blue bars*) conformations. Although a fewer number of NMR signals were visible in the complex, their secondary chemical shifts were similar to those of the D-state of IscU. The chemical shifts of the S- and D- states of IscU are from Biological Magnetic Resonance Data Bank accession numbers 17836 and 17837, respectively. These results and the chemical shift analysis of the assigned backbone signals of IscU indicate that the protein lacks secondary structure in the complex. *D*, perturbation pattern mapped onto the solution structure of the S-state of apo-IscU (Protein Data Bank 2L4X). IscU residues whose ^{1}H-^{15}N NMR cross-peaks were observed in the IscU-HscA complex are colored *green*; residues whose cross-peaks broadened and were not observed by the interaction with HscA are colored *red*; and residues whose cross-peaks were not observed or assigned are colored *black*.

interact strongly with the S-state of IscU and that the S → D equilibrium must be perturbed to the D-state to form the complex.

HscA SBD Preferentially Binds and Stabilizes the D-state of Apo-IscU—Studies of *E. coli* DnaK (31, 32) and the x-ray structure of the HscA SBD complexed with the nonapeptide E^{98}LPPVKIHC^{106} (22) have shown that that the isolated SBD binds its substrate. We carried out titration experiments similar to those described above, but with the HscA SBD in place of full-length HscA and with [U-^{15}N,frac-^{2}H]IscU, whose backbone ^{1}H-^{15}N HSQC signals broadened much less than those of [U-^{15}N]IscU in the complex. The results demonstrated that the HscA SBD binds to and stabilizes a D-like state of IscU (Fig. 5). The addition of 2 eq of the HscA SBD led to the disappearance of the S-state peaks of apo-IscU. We conclude that the HscA SBD, like full-length HscA, binds to and stabilizes a D-like state of IscU. With the smaller complex containing fractionally deuterated IscU, we were able to resolve a few peaks (indicated by *arrows* in Fig. 5) that appear likely to correspond to residues of IscU directly involved in the binding interface.

Summary of Effects of Protein and Ligand Binding on the Conformational State of IscU—We found that the ^{1}H-^{15}N cross-peaks from the backbone of Lys-128 in ^{15}N TROSY-HSQC spectra of [U-^{15}N]apo-IscU provide a useful monitor for following the conformational state of IscU in protein-protein complexes (Fig. 6*A*). Although Lys-128 is located in the disordered C-terminal region of IscU, it nonetheless exhibits separate peaks corresponding to the S- and D-states of apo-IscU. In addition, because the residue is located in a highly disordered region, the intensities of its signals are minimally affected by the molecular size of the complex; and from its location and poor sequence conservation (16), it is unlikely that Lys-128 is involved in interactions with HscB or HscA. We measured the volumes of the peaks assigned to the S- and D-states under a variety of conditions and used these to calculate the following: percent structured (%S) = (100 × [S])/([S] + [D]) (Fig. 6*B*). %S ≈ 84 for 0.3 mM IscU alone. Upon the addition of equimolar HscB, %S increased to 93. Equimolar IscU + HscA had %S = 51, as did equimolar IscU + HscA-ADP. Equimolar IscU +

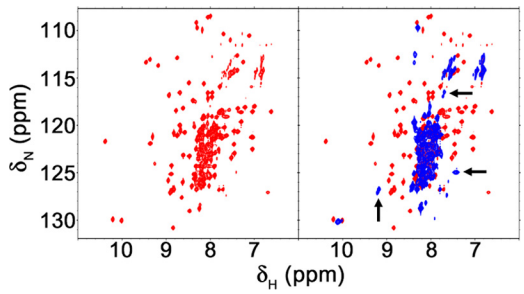

FIGURE 5. **Isolated SBD of HscA also binds and stabilizes the D-state of IscU.** *Left panel*, two-dimensional ^{15}N TROSY-HSQC spectrum of [U-^{15}N,frac-^{2}H]apo-IscU alone (*red*). *Right panel*, two-dimensional ^{15}N TROSY-HSQC spectrum of [U-^{15}N,frac-^{2}H]apo-IscU and the presence of 2 eq of the unlabeled HscA SBD (*blue*) overlaid on the spectrum of apo-IscU alone (*red*). Peaks from the S-state of IscU are not seen in the spectrum of the complex. Most of the peaks in the complex resemble those of the D-state of IscU. However, a few new peaks at new positions (marked with *arrows*) appear in the spectrum of the complex; they likely correspond to IscU residues in the binding interface.

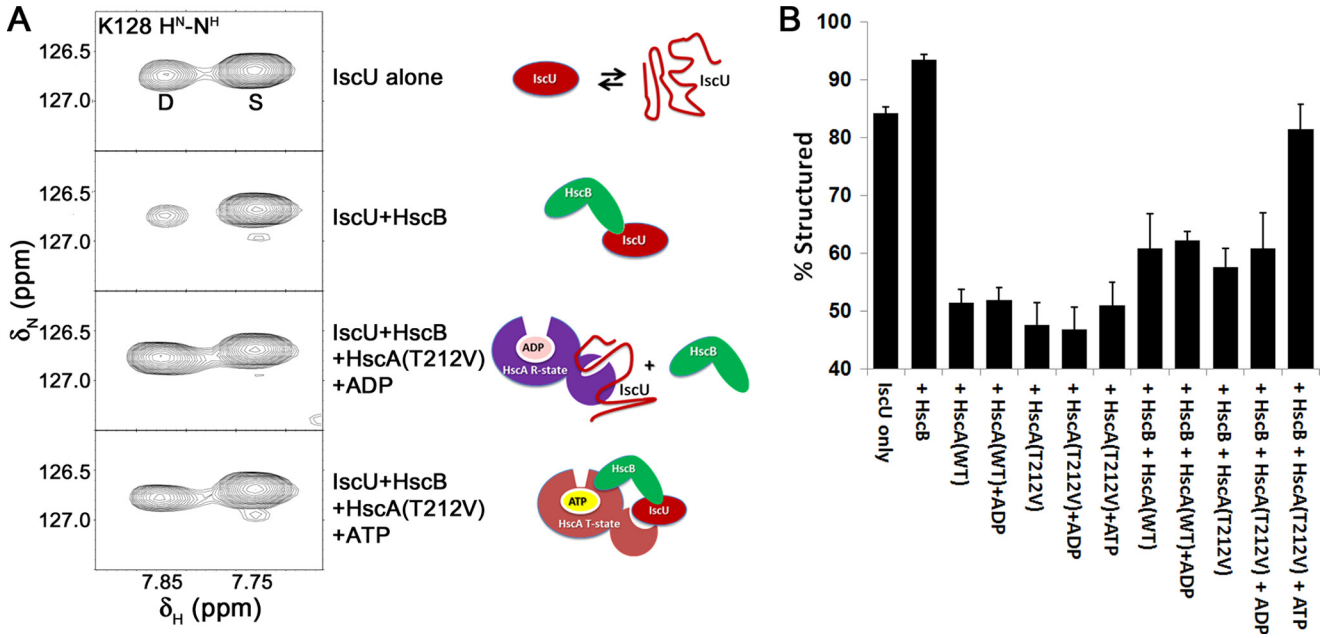

FIGURE 6. **Conformational states of IscU under conditions mimicking various steps in the iron-sulfur cluster transfer mechanism.** *A*, backbone ^{1}H-^{15}N NMR peaks of Lys-128 corresponding to the D- and S-states of IscU. In each panel, the peak from the D-state is on the *left*, and that from the S-state is on the *right*. *First panel*, [U-^{15}N]apo-IscU alone; *second panel*, equimolar [U-^{15}N]apo-IscU and HscB; *third panel*, equimolar [U-^{15}N]apo-IscU, HscB, and HscA(T212V) in the presence of excess ADP; *fourth panel*, equimolar [U-^{15}N]apo-IscU, HscB, and HscA(T212V) in the presence of excess ATP. To the *right* of each panel is a schematic figure (adapted from Fig. 1) representing the step being mimicked. *B*, %S IscU calculated from the volume ratios of the Lys-128 peaks of [U-^{15}N]apo-IscU under the conditions shown. All samples contained 0.3 mM [U-^{15}N]apo-IscU plus equimolar amounts of other proteins on indicated at the *horizontal axis*. Excess ADP or ATP was added as indicated. The %S values were calculated as described in the text. At least two independent measurements were made to test reproducibility and to estimate errors (S.D. shown by *error bars*).

HscA(T212V) in the absence or presence of ADP yielded %S = 47. %S increased to 51 for IscU + HscA(T212V) + ATP. Equimolar IscU + HscB + HscA had %S = 60. This value remained about the same when wild-type HscA was substituted by HscA(T212V) or when ADP was added to equimolar IscU + HscB + HscA(T212V). However, %S increased to a value similar to that for IscU alone when ADP in the previous mixture was replaced by ATP. We used HscA(T212V), which lacks ATPase activity, as a surrogate for HscA in this experiment because the addition of IscU to HscA-ATP led to rapid ATP hydrolysis (data not shown).

These results confirmed our earlier finding that HscB binds preferentially to the S-state of IscU (16). The stabilizing effect of HscB is negated by HscA, which interacts preferentially with the D-state both alone and in its ADP complex. As noted above, the results establish that HscA-ATP fails to interact preferentially with either state of IscU.

DISCUSSION

An earlier model (30) postulated that cluster transfer occurs following the exchange of ADP with ATP, leading to release of holo-IscU from HscA. The results presented here show that cluster transfer instead is coupled to the hydrolysis of ATP bound to HscA with conversion of HscA from the T-state to the R-state, which binds IscU (Fig. 1). HscA-ADP binds to the D-state of IscU, and IscU in the complex is disordered and incapable of retaining the Fe-S cluster.

The results presented here, along with those published earlier (16), demonstrate that HscB binds preferentially to the S-state of IscU, *i.e.* the conformational state of IscU in its [2Fe-2S] complex. The HscB-IscU-[2Fe-2S] complex then binds to HscA through interaction of the J-domain of HscB with the nucleic acid domain of HscA. However, because we found that the ATP-bound state of HscA failed to interact strongly with either the S- or D-state of IscU, we postulate that hydrolysis of ATP to ADP is necessary for initiating the interaction of HscA with IscU.

In the IscU-[2Fe-2S] complex, the side chains of His-105 and Cys-106 ligate different iron atoms, and the backbone conformation of the recognition peptide (E^{98}LPPVKIHC^{106}) is very different from its conformation when complexed to the HscA SBD (22). We found that, when bound to HscA, IscU residues flanking the recognition peptide exhibited NMR chemical shifts very similar to those of the D-state of IscU (Fig. 4). We conclude that IscU must undergo the S → D conversion to interact with HscA.

We speculate here that the attack of cysteinyl side chains from an acceptor protein on iron atoms of the IscU-bound Fe-S cluster is the event that triggers both ATP hydrolysis and the disordering of the recognition peptide that allows it to bind to HscA-ADP. In a possible scenario, which has yet to be tested, attack of two Cys residues from the acceptor protein on the two iron atoms of the [2Fe-2S] cluster displaces IscU ligands His-105 and Cys-106 in the recognition peptide. This reaction distorts the conformation of IscU and changes its interaction with HscB, which in turn transmits the change to the nucleotide-binding domain of HscA so as to turn on ATP hydrolysis. The ADP-bound form of HscA interacts with the recognition peptide and stabilizes the D-state of IscU, which releases the Fe-S

cluster completely along with HscB. The net result is complete irreversible transfer of the cluster to the acceptor protein. Such a mechanism would have the benefit that ATP hydrolysis is triggered only when an acceptor protein is in place to receive the cluster, thus avoiding idle cycles of ATP hydrolysis and loss of the cluster without transfer.

It has been shown that Hsp70 proteins can disentangle nonnative regions of a misfolded protein and assist folding to its native fold by means of an ATP-dependent cycle (33–35). Two mechanisms have been proposed to explain this effect: Hsp70 acts as an "unfoldase" by directly recognizing and unfolding a misfolded protein substrate and then releasing it (36), and/or Hsp70 acts as a "holdase" that prevents a polypeptide chain from being misfolded or aggregated by holding susceptible regions of the substrate (37). Our finding that HscA decreases the D → S rate and binds to and stabilizes the disordered state of IscU implies that it acts as a holdase, and our finding that HscA has no effect on the S → D rate and binds poorly to the structured state of IscU argues against its acting as an unfoldase. A major difference between HscA and the other Hsp70 proteins is that HscA is specifically targeted to the $L^{99}PPVK^{103}$ motif of IscU, whereas Hsp70 proteins usually have a wide range of substrate specificity. Our chemical shift perturbation study suggests that HscA may have a second recognition motif, $V^{73}TEWVKG^{79}$ (denoted by an *asterisk* in Fig. 4*B*). We identified signals from IscU in the complex (Fig. 5) that appear to correspond to residues directly involved in the binding interaction with HscA. Follow-up studies are under way to assign these signals.

IscU differs from the class of intrinsically disordered proteins that (partially) fold upon binding a protein or other ligand (38) in that the two states (D and S) are nearly equally populated in the absence of ligand. IscU belongs instead to the class of proteins termed metamorphic proteins (39), which, under physiological conditions, are capable of populating two different folds that fulfill different functions. Founding members of this class include lymphotactin (40, 41) and Mad2 (42). The two states of metamorphic proteins differ by <2 kcal/mol. Whereas the alternative states of lymphotactin and Mad2 are monomers and dimers, both states of IscU are monomeric. The co-evolution of stable alternative conformations in metamorphic proteins has yet to be explored in detail.

Acknowledgments—We thank Drs. Larry E. Vickery and Dennis T. Ta (University of California, Irvine) for providing expression plasmids of full-length WT HscA and the HscA SBD and Brian F. Volkman (Medical College of Wisconsin) for helpful discussions.

REFERENCES

1. Py, B., and Barras, F. (2010) Building Fe-S proteins: bacterial strategies. *Nat. Rev. Microbiol.* **8,** 436–446
2. Lill, R., and Mühlenhoff, U. (2008) Maturation of iron-sulfur proteins in eukaryotes: mechanisms, connected processes, and diseases. *Annu. Rev. Biochem.* **77,** 669–700
3. Johnson, D. C., Dean, D. R., Smith, A. D., and Johnson, M. K. (2005) Structure, function, and formation of biological iron-sulfur clusters. *Annu. Rev. Biochem.* **74,** 247–281
4. Chandramouli, K., and Johnson, M. K. (2006) HscA and HscB stimulate [2Fe-2S] cluster transfer from IscU to apoferredoxin in an ATP-dependent reaction. *Biochemistry* **45,** 11087–11095
5. Bonomi, F., Iametti, S., Ta, D., and Vickery, L. E. (2005) Multiple turnover transfer of [2Fe-2S] clusters by the iron-sulfur cluster assembly scaffold proteins IscU and IscA. *J. Biol. Chem.* **280,** 29513–29518
6. Zheng, L., Cash, V. L., Flint, D. H., and Dean, D. R. (1998) Assembly of iron-sulfur clusters. Identification of an *iscSUA-hscBA-fdx* gene cluster from *Azotobacter vinelandii*. *J. Biol. Chem.* **273,** 13264–13272
7. Silberg, J. J., Tapley, T. L., Hoff, K. G., and Vickery, L. E. (2004) Regulation of the HscA ATPase reaction cycle by the co-chaperone HscB and the iron-sulfur cluster assembly protein IscU. *J. Biol. Chem.* **279,** 53924–53931
8. Hoff, K. G., Ta, D. T., Tapley, T. L., Silberg, J. J., and Vickery, L. E. (2002) Hsc66 substrate specificity is directed toward a discrete region of the iron-sulfur cluster template protein IscU. *J. Biol. Chem.* **277,** 27353–27359
9. Hoff, K. G., Cupp-Vickery, J. R., and Vickery, L. E. (2003) Contributions of the LPPVK motif of the iron-sulfur template protein IscU to interactions with the Hsc66-Hsc20 chaperone system. *J. Biol. Chem.* **278,** 37582–37589
10. Silberg, J. J., Hoff, K. G., Tapley, T. L., and Vickery, L. E. (2001) The Fe-S assembly protein IscU behaves as a substrate for the molecular chaperone Hsc66 from *Escherichia coli*. *J. Biol. Chem.* **276,** 1696–1700
11. Hoff, K. G., Silberg, J. J., and Vickery, L. E. (2000) Interaction of the iron-sulfur cluster assembly protein IscU with the Hsc66-Hsc20 molecular chaperone system of *Escherichia coli*. *Proc. Natl. Acad. Sci. U.S.A.* **97,** 7790–7795
12. Füzéry, A. K., Oh, J. J., Ta, D. T., Vickery, L. E., and Markley, J. L. (2011) Three hydrophobic amino acids in *Escherichia coli* HscB make the greatest contribution to the stability of the HscB-IscU complex. *BMC Biochem.* **12,** 3
13. Olsson, A., Lind, L., Thornell, L. E., and Holmberg, M. (2008) Myopathy with lactic acidosis is linked to chromosome 12q23.3-24.11 and caused by an intron mutation in the *ISCU* gene resulting in a splicing defect. *Hum. Mol. Genet.* **17,** 1666–1672
14. Mochel, F., Knight, M. A., Tong, W. H., Hernandez, D., Ayyad, K., Taivassalo, T., Andersen, P. M., Singleton, A., Rouault, T. A., Fischbeck, K. H., and Haller, R. G. (2008) Splice mutation in the iron-sulfur cluster scaffold protein ISCU causes myopathy with exercise intolerance. *Am. J. Hum. Genet.* **82,** 652–660
15. Nordin, A., Larsson, E., Thornell L. E., and Holmberg, M. (2011) Tissue-specific splicing of ISCU results in a skeletal muscle phenotype in myopathy with lactic acidosis, while complete loss of ISCU results in early embryonic death in mice. *Hum. Genet.* **129,** 371–378
16. Kim, J. H., Füzéry, A. K., Tonelli, M., Ta, D. T., Westler, W. M., Vickery, L. E., and Markley, J. L. (2009) Structure and dynamics of the iron-sulfur cluster assembly scaffold protein IscU and its interaction with the co-chaperone HscB. *Biochemistry* **48,** 6062–6071
17. Shimomura, Y., Wada, K., Fukuyama, K., and Takahashi, Y. (2008) The asymmetric trimeric architecture of [2Fe-2S] IscU: implications for its scaffolding during iron-sulfur cluster biosynthesis. *J. Mol. Biol.* **383,** 133–143
18. Ramelot, T. A., Cort, J. R., Goldsmith-Fischman, S., Kornhaber, G. J., Xiao, R., Shastry, R., Acton, T. B., Honig, B., Montelione, G. T., and Kennedy, M. A. (2004) Solution NMR structure of the iron-sulfur cluster assembly protein U (IscU) with zinc bound at the active site. *J. Mol. Biol.* **344,** 567–583
19. Kim, J. H., Tonelli, M., and Markley, J. L. (2012) Disordered form of the scaffold protein IscU is the substrate for iron-sulfur cluster assembly on cysteine desulfurase. *Proc. Natl. Acad. Sci. U.S.A.* **109,** 454–459
20. Otten, R., Chu, B., Krewulak, K. D., Vogel, H. J., and Mulder, F. A. (2010) Comprehensive and cost-effective NMR spectroscopy of methyl groups in large proteins. *J. Am. Chem. Soc.* **132,** 2952–2960
21. Vickery, L. E., Silberg, J. J., and Ta, D. T. (1997) Hsc66 and Hsc20, a new heat shock cognate molecular chaperone system from *Escherichia coli*. *Protein Sci.* **6,** 1047–1056
22. Cupp-Vickery, J. R., Peterson, J. C., Ta, D. T., and Vickery, L. E. (2004) Crystal structure of the molecular chaperone HscA substrate-binding domain complexed with the IscU recognition peptide ELPPVKIHC. *J. Mol. Biol.* **342,** 1265–1278

23. Delaglio, F., Grzesiek, S., Vuister, G. W., Zhu, G., Pfeifer, J., and Bax, A. (1995) NMRPipe: a multidimensional spectral processing system based on UNIX pipes. *J. Biomol. NMR* **6,** 277–293
24. Goddard, T. D., and Kneller, D. G. (2008) *SPARKY 3*, University of California, San Francisco
25. Chylla, R. A., Hu, K., Ellinger, J. J., and Markley, J. L. (2011) Deconvolution of two-dimensional NMR spectra by fast maximum likelihood reconstruction: application to quantitative metabolomics. *Anal. Chem.* **83,** 4871–4880
26. Montelione, G. T., and Wagner, G. (1989) 2D chemical exchange NMR spectroscopy by proton-detected heteronuclear correlation. *J. Am. Chem. Soc.* **111,** 3096–3098
27. Silberg, J. J., and Vickery, L. E. (2000) Kinetic characterization of the ATPase cycle of the molecular chaperone Hsc66 from *Escherichia coli*. *J. Biol. Chem.* **275,** 7779–7786
28. Barthel, T. K., Zhang, J., and Walker, G. C. (2001) ATPase-defective derivatives of *Escherichia coli* DnaK that behave differently with respect to ATP-induced conformational change and peptide release. *J. Bacteriol.* **183,** 5482–5490
29. Taneva, S. G., Moro, F., Velázquez-Campoy, A., and Muga, A. (2010) Energetics of nucleotide-induced DnaK conformational states. *Biochemistry* **49,** 1338–1345
30. Bonomi, F., Iametti, S., Morleo, A., Ta, D., and Vickery, L. E. (2008) Studies on the mechanism of catalysis of iron-sulfur cluster transfer from IscU-[2Fe-2S] by HscA/HscB chaperones. *Biochemistry* **47,** 12795–12801
31. Swain, J. F., Dinler, G., Sivendran, R., Montgomery, D. L., Stotz, M., and Gierasch, L. M. (2007) Hsp70 chaperone ligands control domain association via an allosteric mechanism mediated by the interdomain linker. *Mol. Cell* **26,** 27–39
32. Rist, W., Graf, C., Bukau, B., and Mayer, M. P. (2006) Amide hydrogen exchange reveals conformational changes in Hsp70 chaperones important for allosteric regulation. *J. Biol. Chem.* **281,** 16493–16501
33. Schröder, H., Langer, T., Hartl, F. U., and Bukau, B. (1993) DnaK, DnaJ, and GrpE form a cellular chaperone machinery capable of repairing heat-induced protein damage. *EMBO J.* **12,** 4137–4144
34. Szabo, A., Langer, T., Schröder, H., Flanagan, J., Bukau, B., and Hartl, F. U. (1994) The ATP hydrolysis-dependent reaction cycle of the *Escherichia coli* Hsp70 system DnaK, DnaJ, and GrpE. *Proc. Natl. Acad. Sci. U.S.A.* **91,** 10345–10349
35. Sharma, S. K., Christen, P., and Goloubinoff, P. (2009) Disaggregating chaperones: an unfolding story. *Curr. Protein Pept. Sci.* **10,** 432–446
36. Sharma, S. K., De los Rios, P., Christen, P., Lustig, A., and Goloubinoff, P. (2010) The kinetic parameters and energy cost of the Hsp70 chaperone as a polypeptide unfoldase. *Nat. Chem. Biol.* **6,** 914–920
37. Slepenkov, S. V., and Witt, S. N. (2002) The unfolding story of the *Escherichia coli* Hsp70 DnaK: is DnaK a holdase or an unfoldase? *Mol. Microbiol.* **45,** 1197–1206
38. Wright, P. E., and Dyson, H. J. (2009) Linking folding and binding. *Curr. Opin. Struct. Biol.* **19,** 31–38
39. Murzin, A. G. (2008) Biochemistry. Metamorphic proteins. *Science* **320,** 1725–1726
40. Kuloğlu, E. S., McCaslin, D. R., Markley, J. L., and Volkman, B. F. (2002) Structural rearrangement of human lymphotactin, a C chemokine, under physiological solution conditions. *J. Biol. Chem.* **277,** 17863–17870
41. Tyler, R. C., Murray, N. J., Peterson, F. C., and Volkman, B. F. (2011) Native state interconversion of a metamorphic protein requires global unfolding. *Biochemistry* **50,** 7077–7079
42. Mapelli, M., Massimiliano, L., Santaguida, S., and Musacchio, A. (2007) The Mad2 conformational dimer: structure and implications for the spindle assembly checkpoint. *Cell* **131,** 730–743